Synthesis, Structure, and Magnetic Properties of Diamagnetic Co(III) ion-based Heterometallic Co^{III}-Ln^{III} (Ln = Dy, Tb, Ho, Er) Complexes

Nandini Barman[a], Purbashree Halder[a], Subrata Mukhopadhyay[a], Björn Schwarz[b], Enrique Colacio,*[c] Rajanikanta Rana[d], Gopalan Rajaraman*[d], and Joydeb Goura*[a,e,f]*

[a]Department of Chemistry, Jadavpur University, Kolkata-700032, India

[b]Karlsruhe Institute of Technology (KIT) – Institute for Applied Materials (IAM), Hermann-von-Helmholtz-Platz 1, 76344 Eggenstein-Leopoldshafen, Germany

[c]Departamento de Química Inorgánica, Facultad de Ciencias, Universidad de Granada, Av. Fuentenueva S/N, 18071 Granada, Spain

[d]Department of Chemistry, Indian Institute of Technology, Bombay, Powai, Mumbai, Maharashtra 400076, India

[e]Department of Chemistry, University of Delhi, Delhi-110007, India

[f]Department of Chemistry, Bangabasi College, Kolkata-700009

Joydeb Goura: jgoura@chemistry.du.ac.in
joydebgoura@gmail.com
bjoern.schwarz@kit.edu
ecolacio@ugr.es
rajaraman@chem.iitb.ac.in

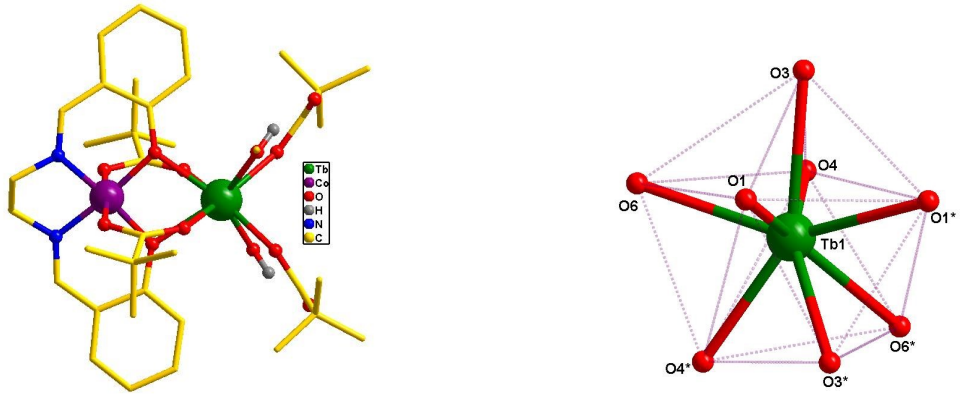

(a) **(b)**

Figure S1. (a) Molecular structure of **2**. All hydrogen atoms have been omitted for clarity. (b) distorted triangular dodecahedron geometry of the terbium center in **2**.

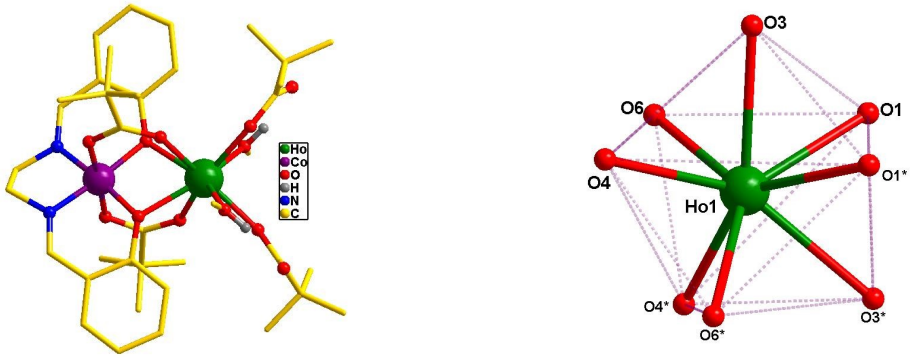

(a) **(b)**

Figure S2. (a) Molecular structure of **3**. All hydrogen atoms have been omitted for clarity. (b) distorted triangular dodecahedron geometry of the terbium center in **3**.

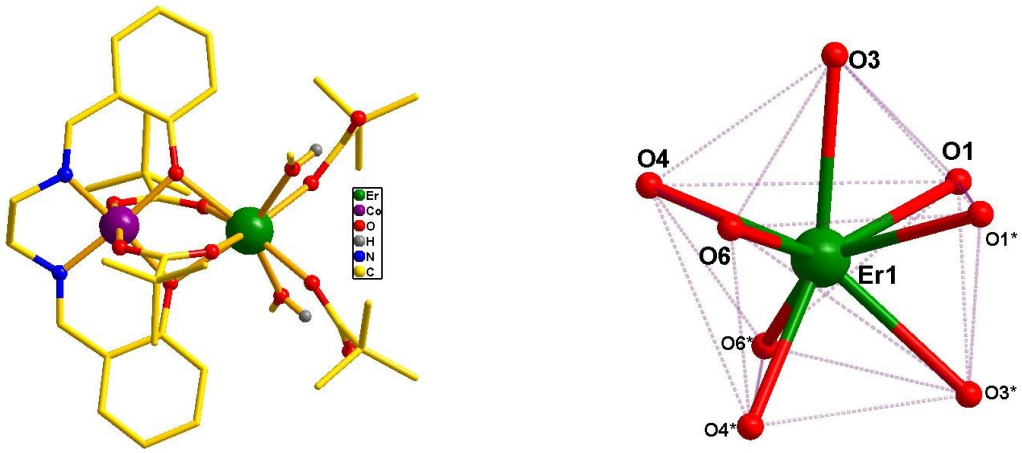

(a) **(b)**

Figure S3. (a) Molecular structure of **4**. All hydrogen atoms have been omitted for clarity. (b) distorted triangular dodecahedron geometry of the terbium center in **4**.

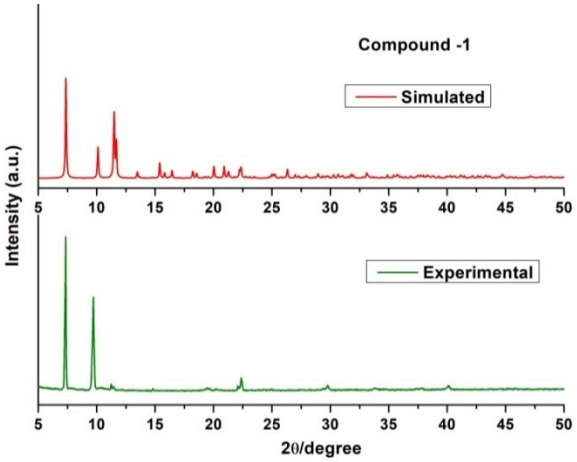

Figure S4. Room temperature PXRD of complex **1**

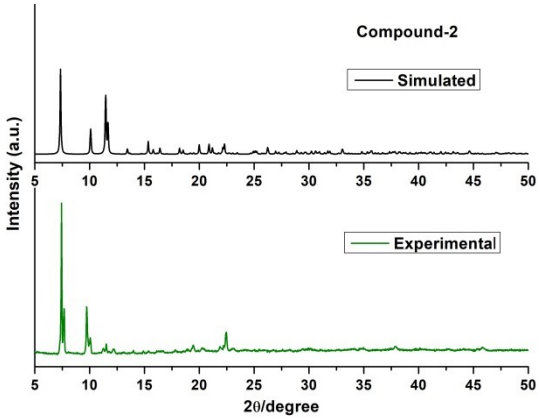

Figure S5. Room temperature PXRD of complex **2**

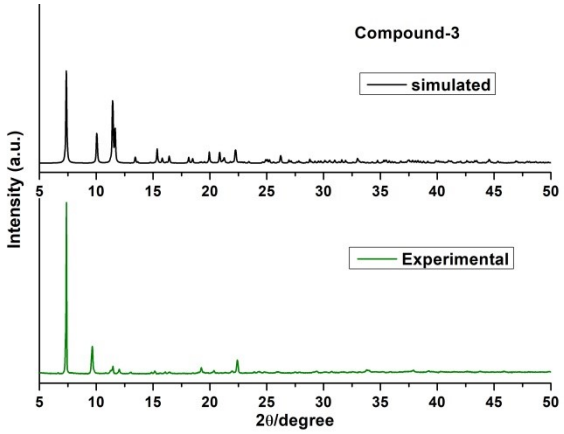

Figure S6. Room temperature PXRD of complex **3**

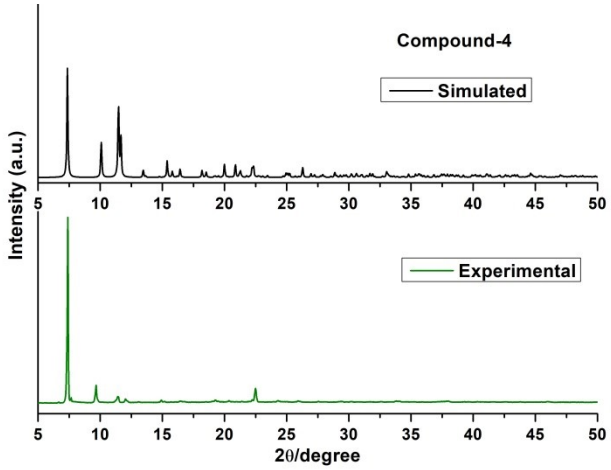

Figure S7. Room temperature PXRD of complex **4**

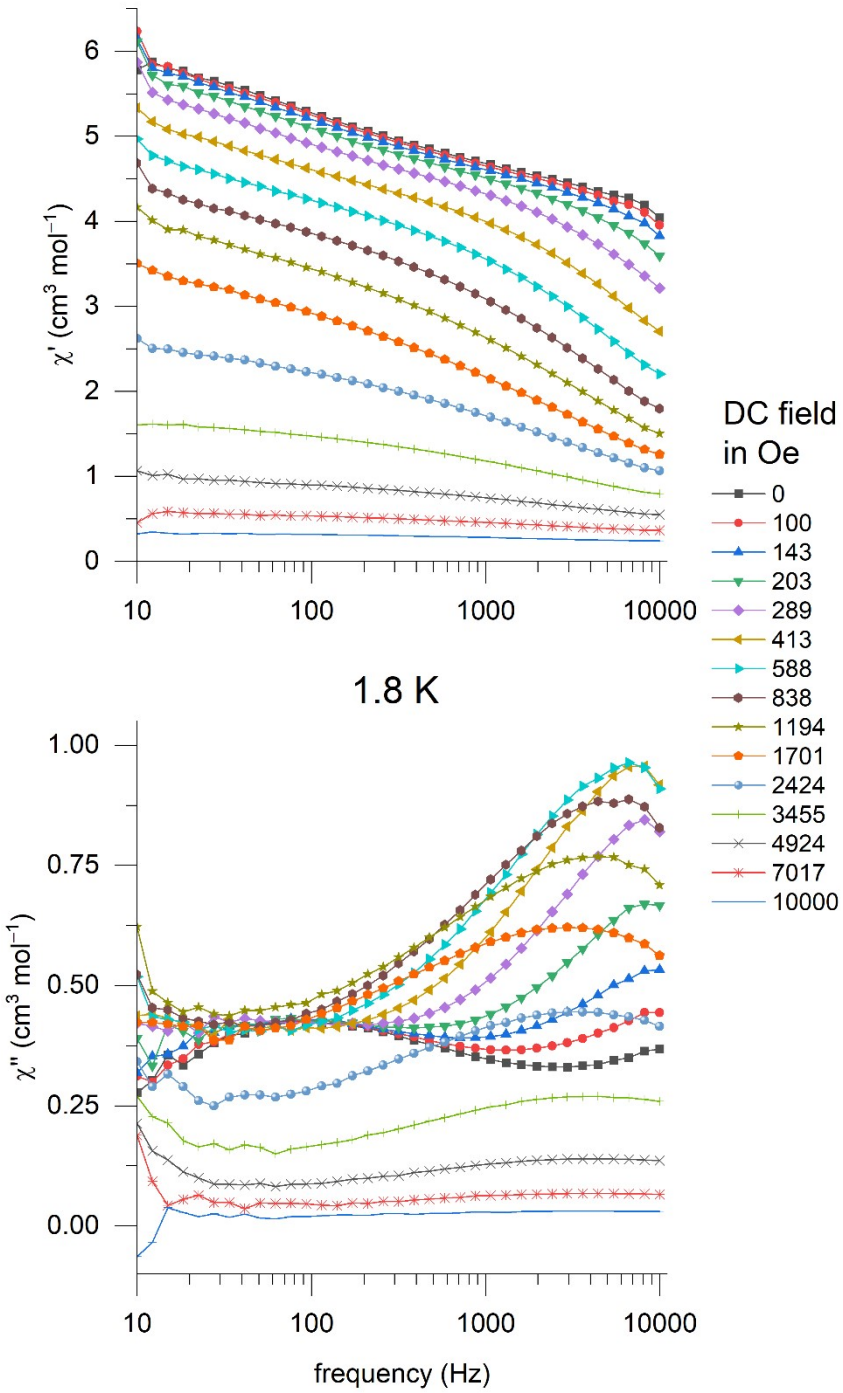

Figure S8. Real part χ′ and imaginary part χ″ of AC susceptibility measured for **1** at various magnetic DC fields at 1.8 K. Errors bars have been omitted for clarity but are smaller than symbols except for the very low frequencies.

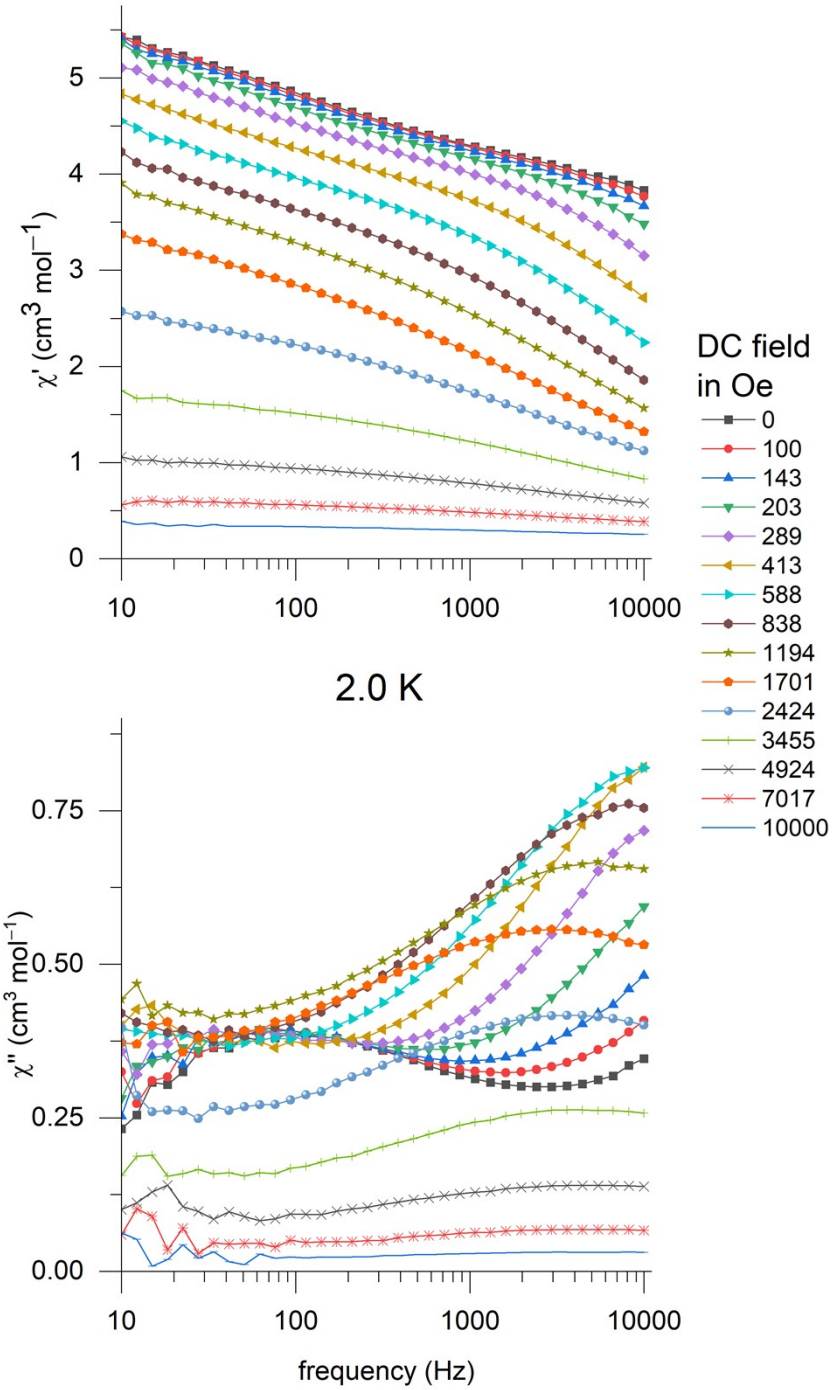

Figure S9. Real part χ' and imaginary part χ'' of AC susceptibility measured for **1** at various magnetic DC fields at 2.0 K. Errors bars have been omitted for clarity but are smaller than symbols except for the very low frequencies.

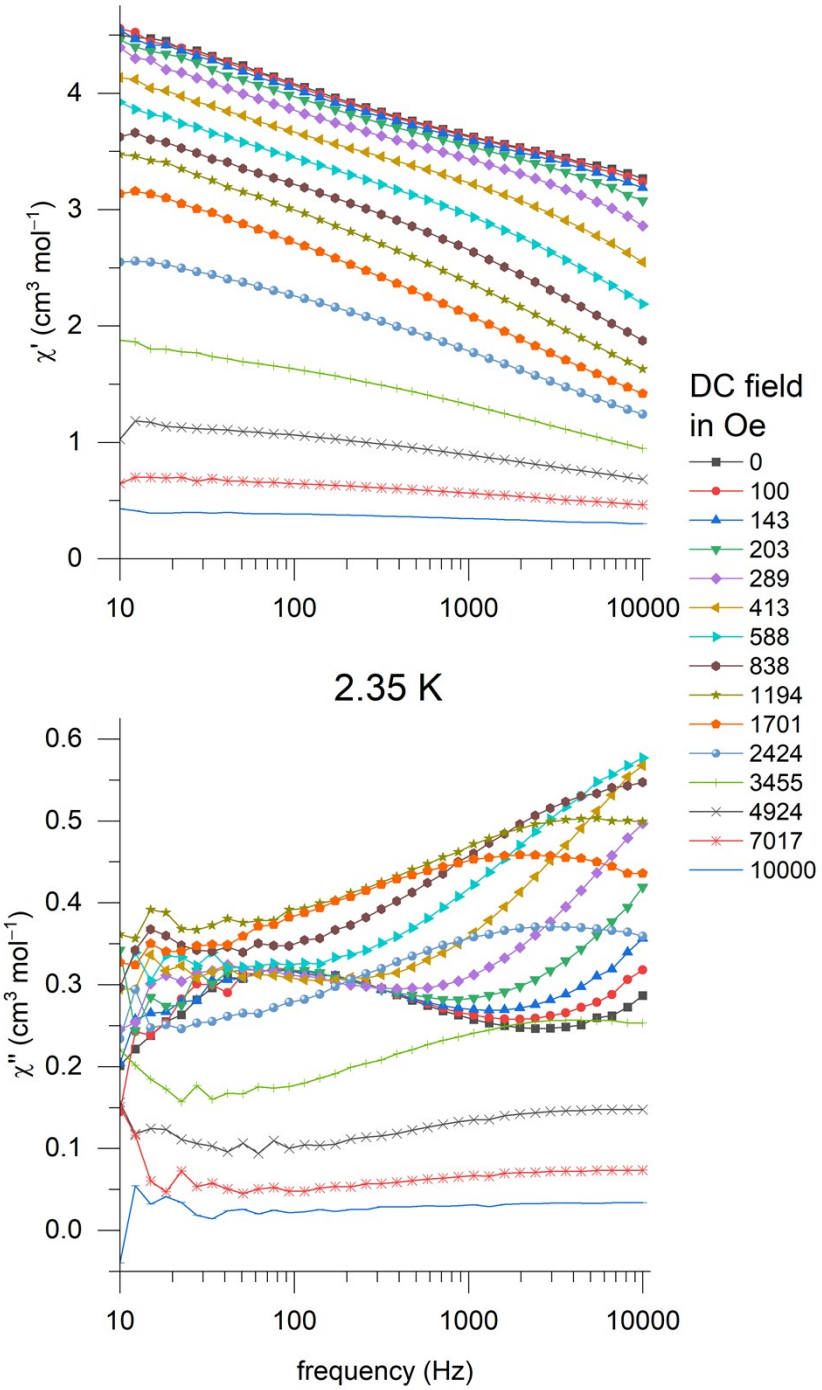

Figure S10. Real part χ' and imaginary part χ'' of AC susceptibility measured for **1** at various magnetic DC fields at 2.35 K. Errors bars have been omitted for clarity but are smaller than symbols except for the very low frequencies.

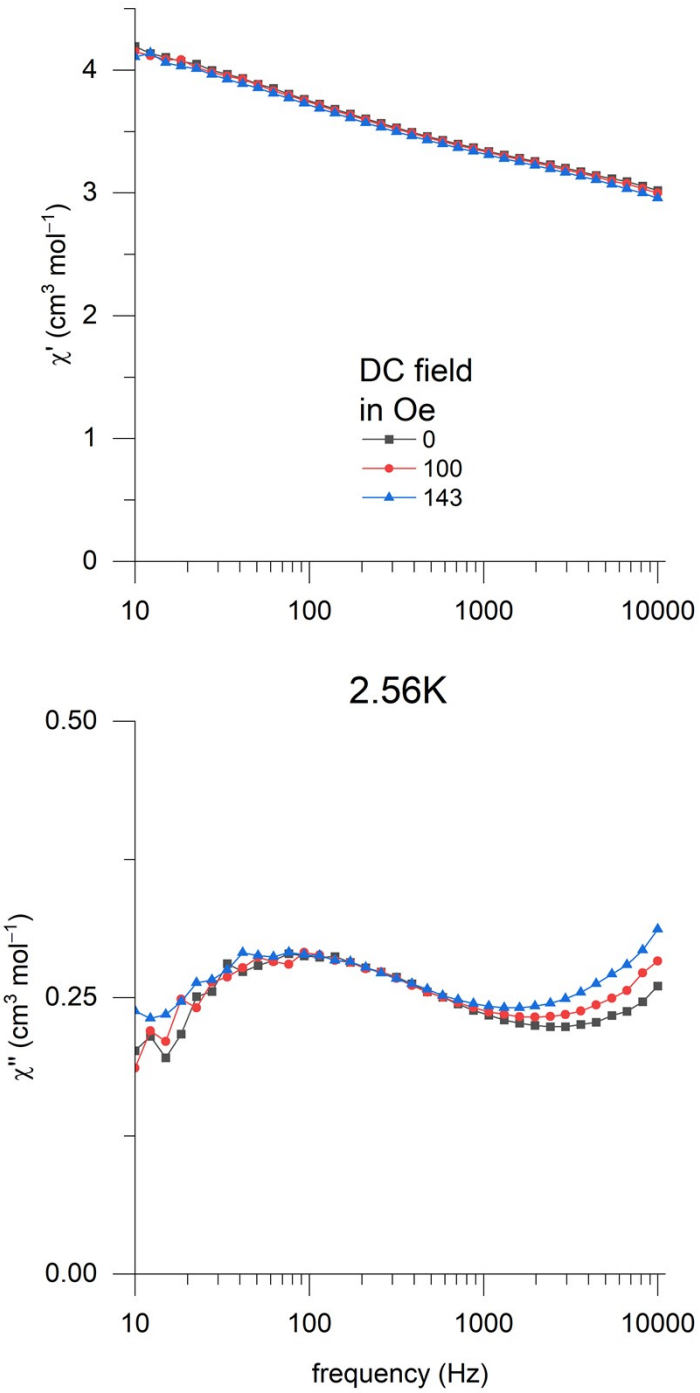

Figure S11. Real part χ' and imaginary part χ'' of AC susceptibility measured for **1** at various magnetic DC fields at 2.56 K. Errors bars have been omitted for clarity but are smaller than symbols except for the very low frequencies.

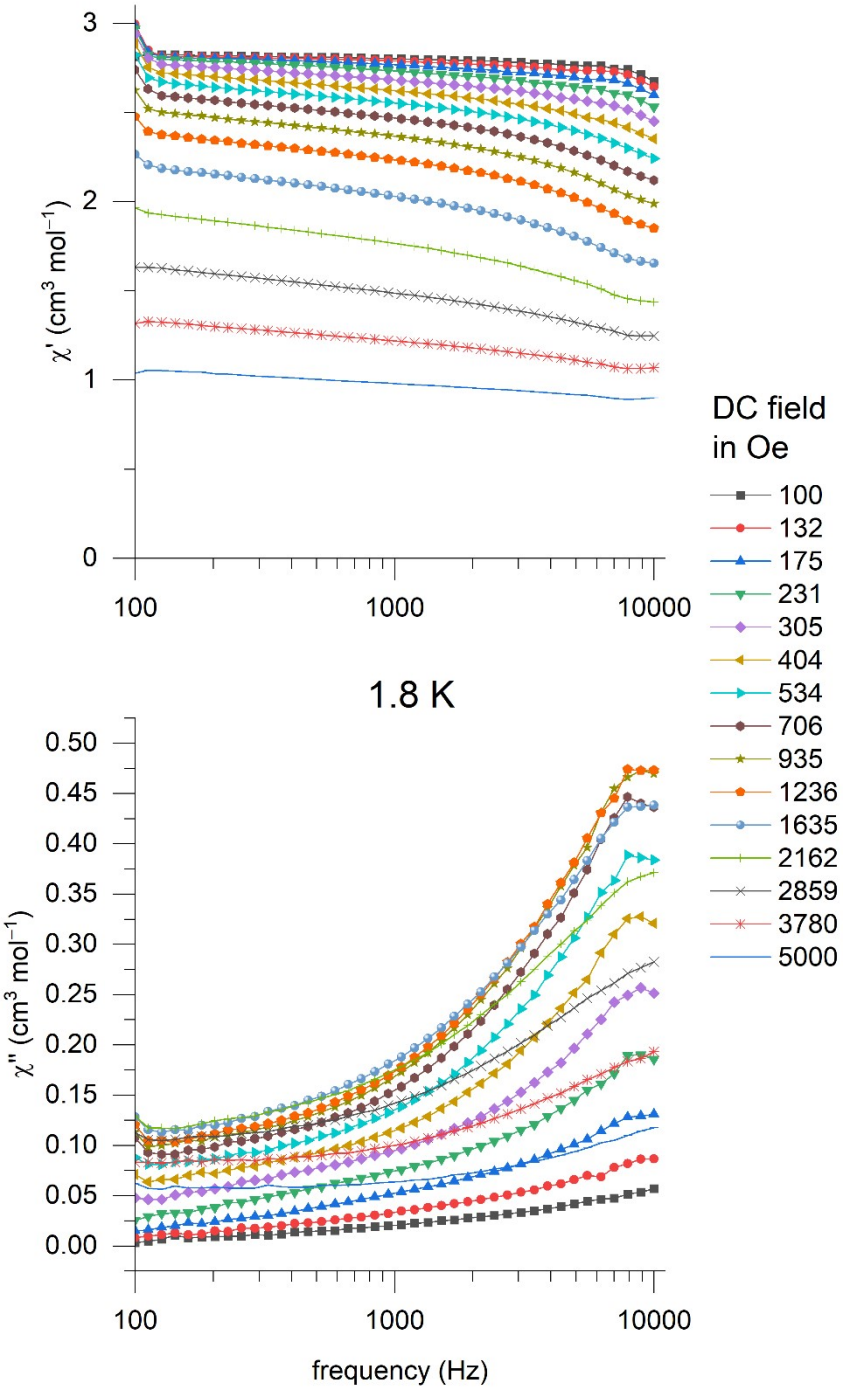

Figure S12. Real part χ' and imaginary part χ'' of *AC* susceptibility measured for **4** at various magnetic *DC* fields (numbers in legend give field in Oe) at 1.8 K. Errors bars have been omitted for clarity but are smaller than symbols except for the very low frequencies.

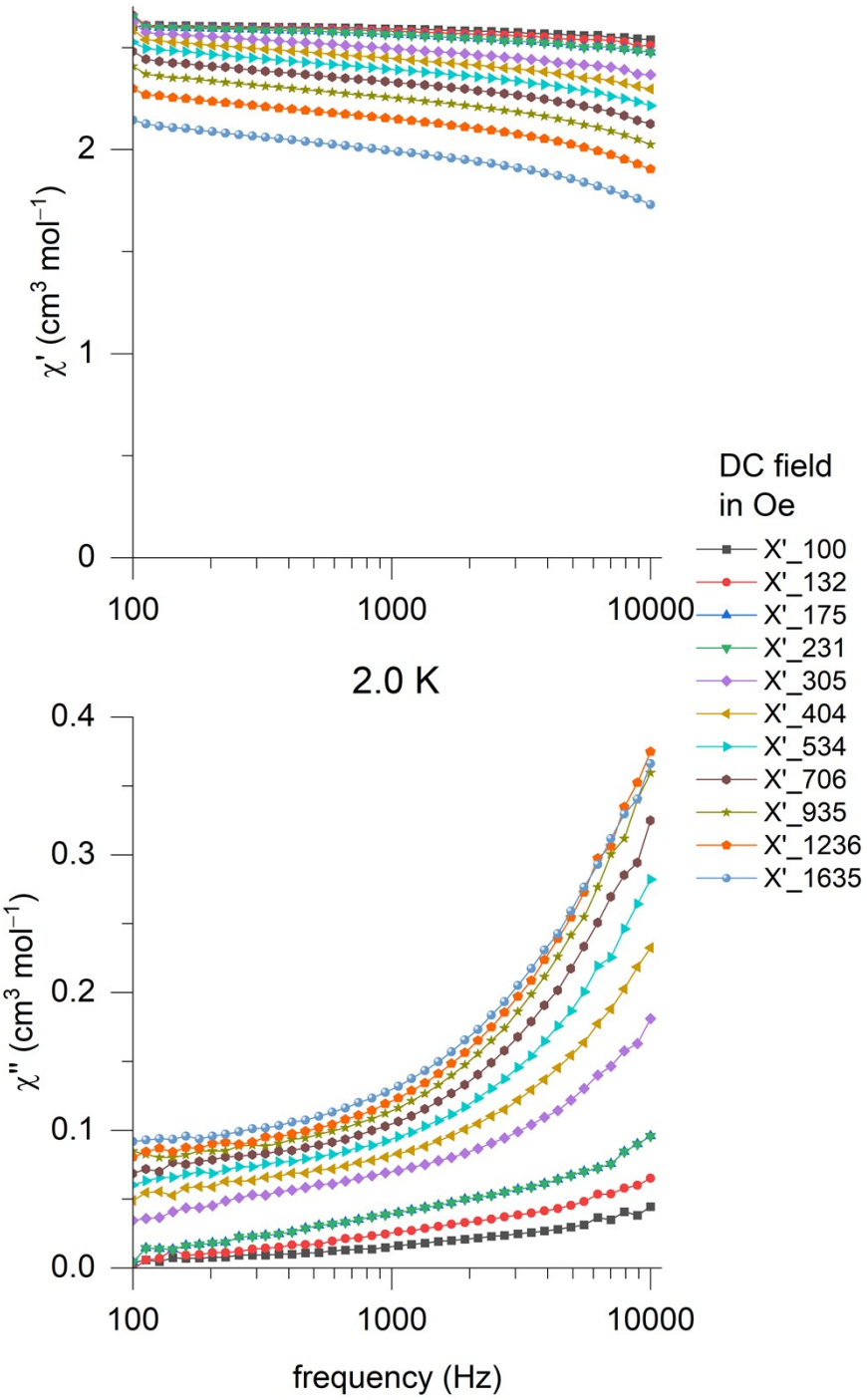

Figure S13. Real part χ' and imaginary part χ'' of *AC* susceptibility measured for **4** at various magnetic *DC* fields up to 1635 Oe at 2.0 K (for legend see measurement at 1.8 K). Errors bars have been ommitted for clarity but are smaller than symbols except for the very low frequencies.

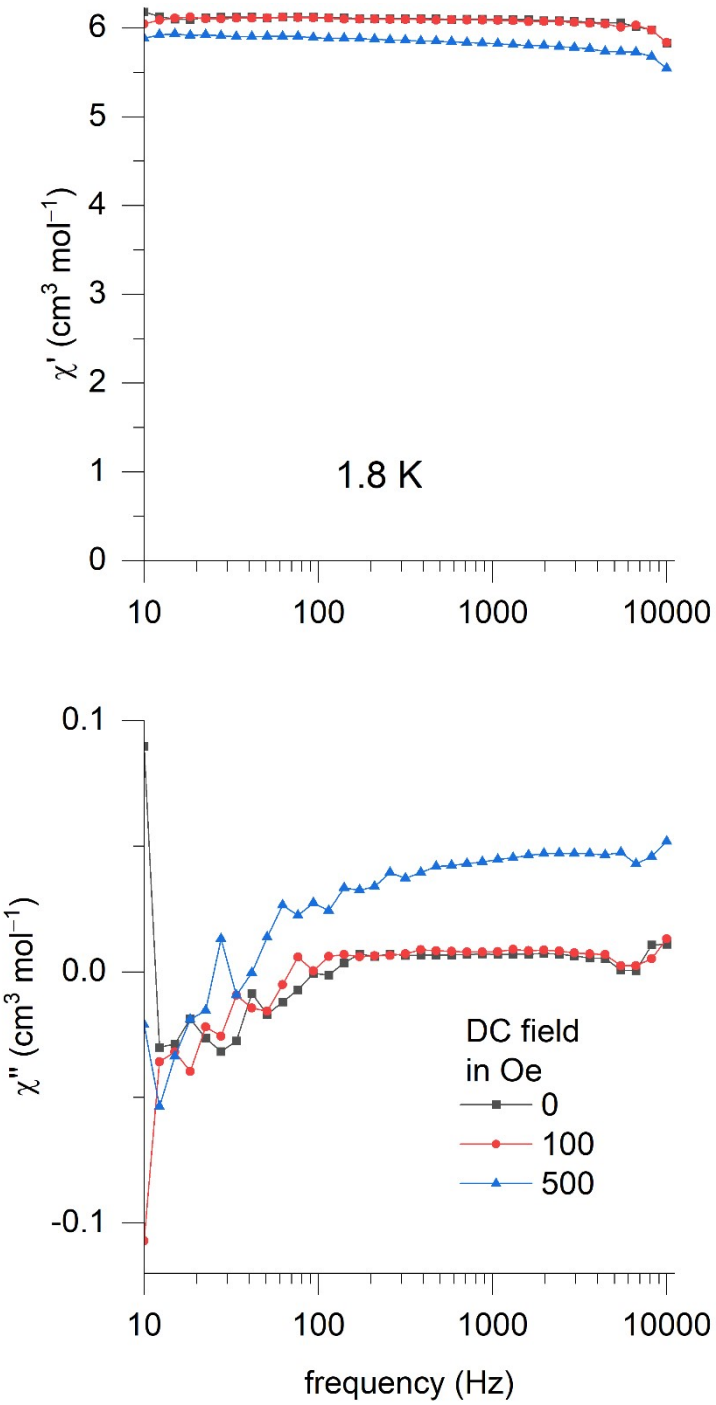

Figure S14. Real part χ' and imaginary part χ'' of *AC* susceptibility measured for **2** at various magnetic *DC* fields at 1.8 K. Errors bars have been omitted for clarity but are smaller than symbols except for the very low frequencies.

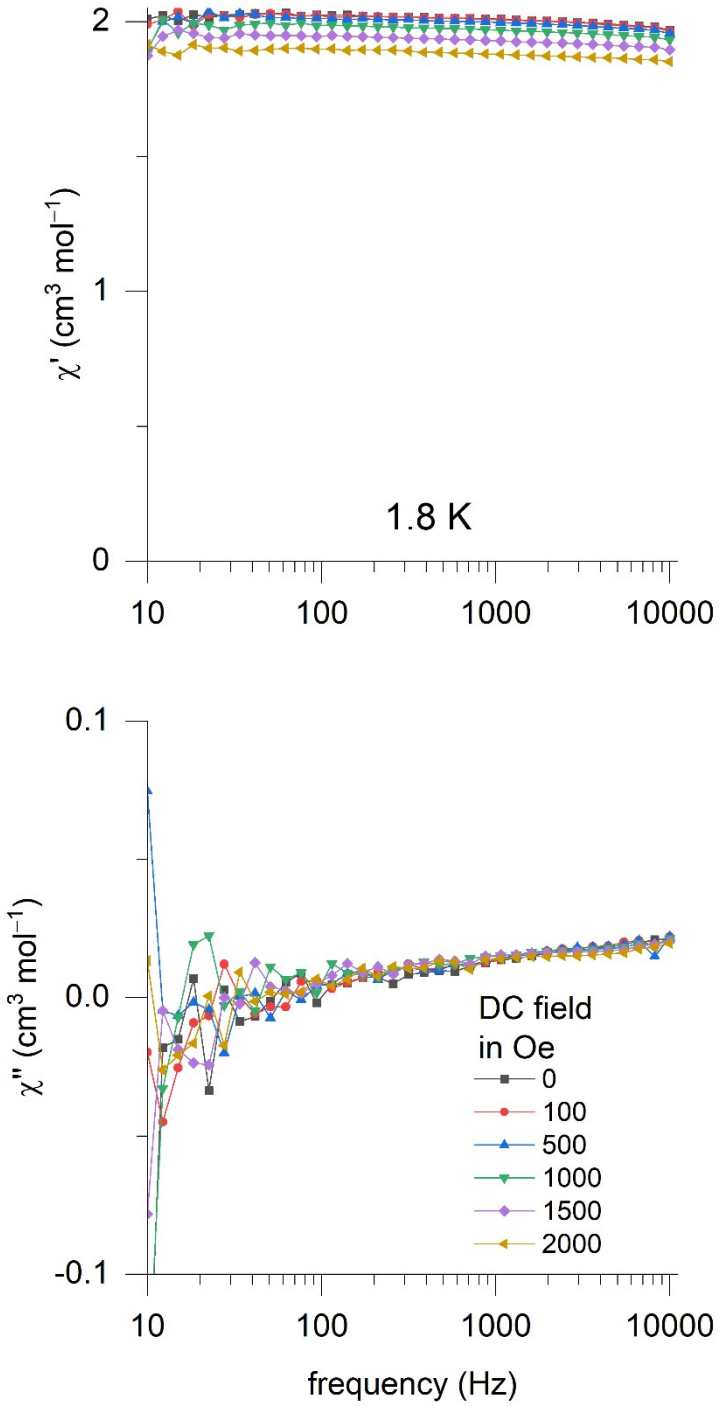

Figure S15. Real part χ' and imaginary part χ'' of *AC* susceptibility measured for **3** at various magnetic *DC* fields at 1.8 K. Errors bars have been omitted for clarity but are smaller than symbols except for the very low frequencies.

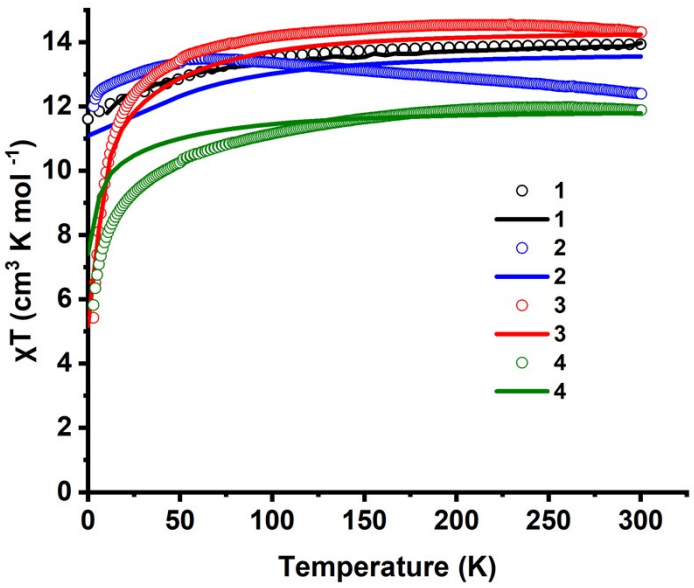

Figure S16. DC magnetometry measurements (circles) and CASSCF calculated (lines) obtained for **1**-**4**: a) χT vs. temperature

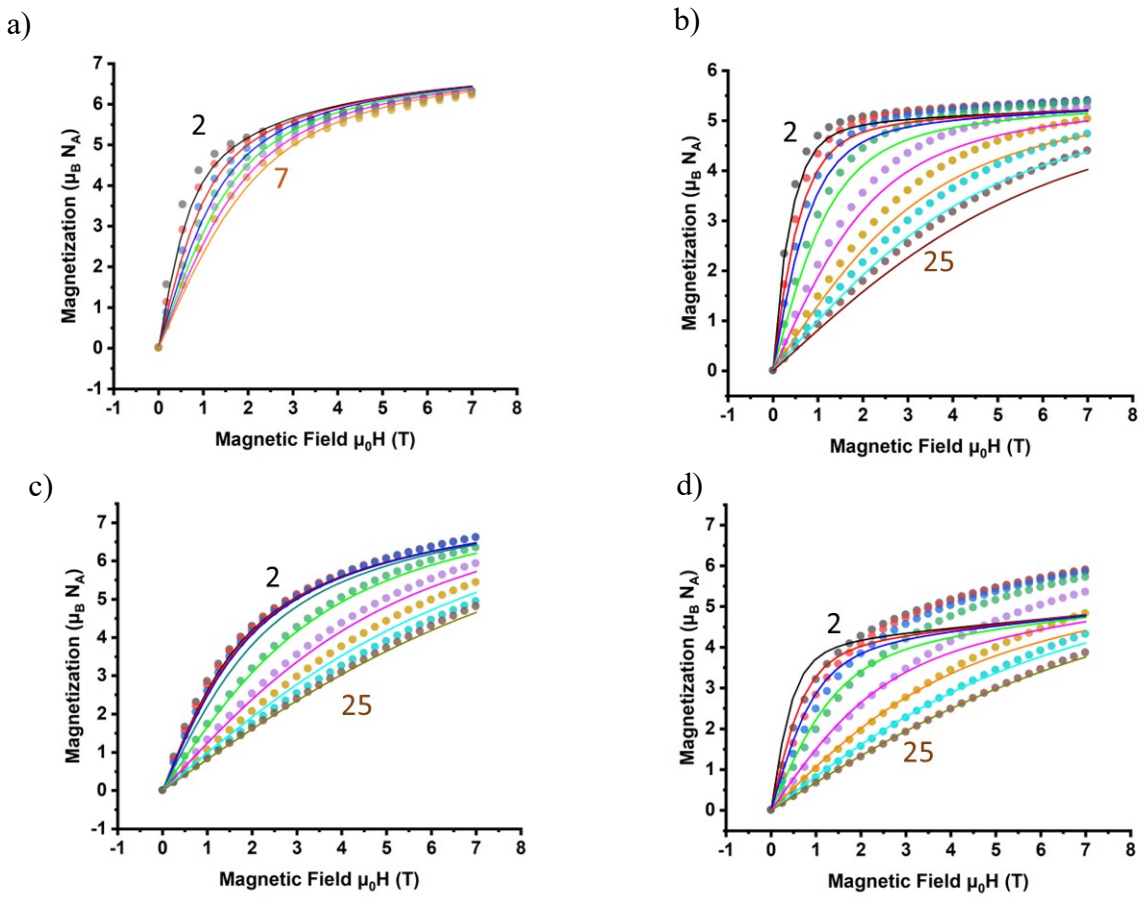

Figure S17. DC magnetometry measurements (circles) and CASSCF calculated (lines) obtained for **1-4:** (a-d) magnetization vs. field. The numbers give the lowest and highest

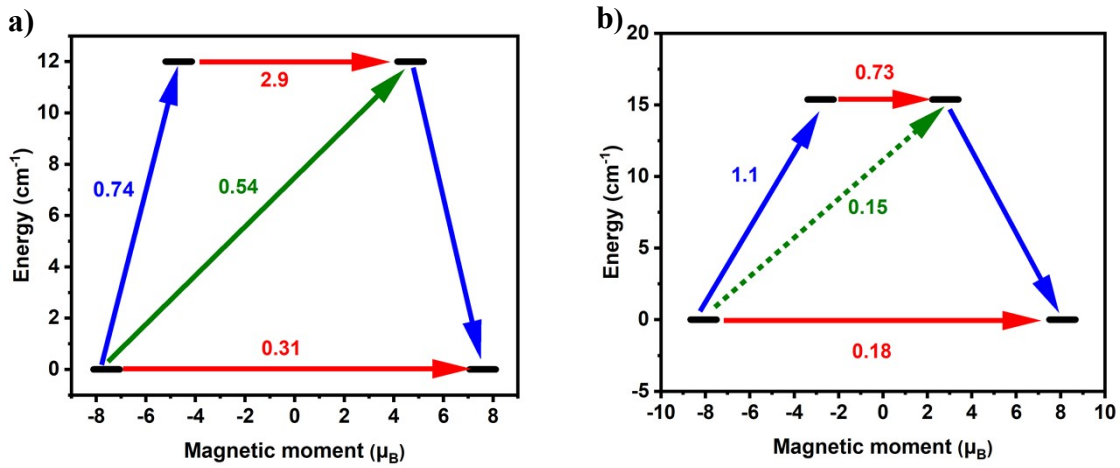

Figure **S18**. Magnetic relaxation in **1** (a) and **4** (b) involves multiple pathways: Kramer's doublet (KD), QTM/TA-QTM via ground/excited states (red arrow), potential Orbach pathway (green arrow), and the most probable relaxation pathway (blue arrow). Associated numbers indicate mean absolute values of corresponding magnetic transition moment matrix elements.

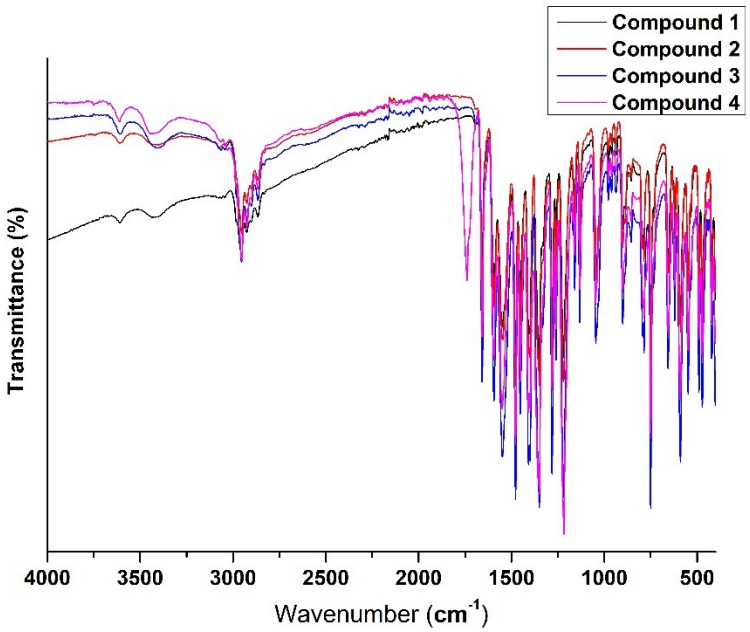

Figure S19. IR spectrum of complexes **1-4**.

Equations

Hamiltonian used for the magnetic models to simulate DC magnetic data:

$$\hat{H} = \hat{H}_{CF} + \hat{H}_{ZEE} \qquad \text{(eqS1)}$$

$\hat{H}_{ZEE}$: Zeeman effect

$\hat{H}_{CF}$: crystal field interaction

$$\hat{H}_{ZEE} = \mu_B \sum_{i=1}^{N} \left(\sigma_i \vec{\hat{L}}_i \cdot \bar{\bar{I}} + \vec{\hat{S}}_i \cdot \bar{\bar{g}}_i \right) \cdot \vec{B}$$

σ_i: orbital reduction parameters

$\vec{\hat{L}}_i$: Vector operator total orbital momentum

$\vec{\hat{S}}_i$: Vector operator total spin orbital momentum

μ_B: Bohr magneton

$\bar{\bar{I}}$: identity matrix

$\bar{\bar{g}}_i$: *g*-tensor

$\vec{B}$: magnetic induction

$$\hat{H}_{CF} = \sum_{i=1}^{N} \sum_{k=2,4,6} \sum_{q=-k}^{k} \sigma_i^k B_{ki}^q \theta_k \hat{O}_{ki}^q$$

B_{ki}^q : Crystal field parameters ($A_{ki}^q \langle r^k \rangle_i$ in Steven's notation)

θ_k: operator equivalent factors

$\hat{O}_{ki}^q$: operator equivalents

Table S1. Sample masses and diamagnetic correction parameters used for DC and AC magnetometry measurements for compounds **1-4**

Compounds	**1**	**2**	**3**	**4**
Lanthanoide	Dysprosium(Dy)	Terbium (Tb)	Holmium (Ho)	Erbium (Er)
Sample mass (mg)	12.4(1)	13.7	13.7(1)	17.1(1)
Molar mass (g mol^{-1})	956	952	958	961
Sample amount (mol)	$1.29707 \cdot 10^{-5}$	$1.43908 \cdot 10^{-5}$	$1.43006 \cdot 10^{-5}$	$1.7794 \cdot 10^{-5}$
Diam. Contrib. pp capsule (emu Oe^{-1})	$-7.71 \cdot 10^{-9}$	$-7.71 \cdot 10^{-9}$	$-7.71 \cdot 10^{-9}$	$-7.71 \cdot 10^{-9}$
Diam. Contrib. closed shells (emu mol^{-1} Oe^{-1})	$-8.3731 \cdot 10^{-5}$	$-8.3731 \cdot 10^{-5}$	$-8.3731 \cdot 10^{-5}$	$-8.4527 \cdot 10^{-5}$

Table S2. BVS calculation for complexes **1-4**.

Compounds	Bond distances r_1		r_0 for Co^{2+}	B			r_0 for Co^{3+}	B		Assigned
1	Co1 - O1*	1.925(4)	1.692	0.37	0.53274		1.680	0.37	0.51574	
	Co1 - O1	1.925(4)	1.692	0.37	0.53274		1.680	0.37	0.51574	
	Co1 - O3*	1.899(3)	1.692	0.37	0.57152		1.680	0.37	0.55328	
	Co1 - O3	1.899(3)	1.692	0.37	0.57152		1.680	0.37	0.55328	
	Co1 - N1	1.892(5)	1.692	0.37	0.58243		1.680	0.37	0.56385	
	Co1 - N1*	1.892(5)	1.692	0.37	0.58243		1.680	0.37	0.56385	
			Sum		**3.37337**		**Sum**		**3.26572**	**Co^{3+}**
2	Co1 - O1*	1.935(5)	1.692	0.37	0.51853		1.680	0.37	0.50198	
	Co1 - O1	1.935(5)	1.692	0.37	0.51853		1.680	0.37	0.50198	
	Co1 - O2	1.906(5)	1.692	0.37	0.56080		1.680	0.37	0.54291	
	Co1 -O2*	1.906(5)	1.692	0.37	0.56080		1.680	0.37	0.54291	
	Co1 - N1*	1.902(6)	1.692	0.37	0.56690		1.680	0.37	0.54881	
	Co1 - N1	1.902(6)	1.692	0.37	0.56690		1.680	0.37	0.54881	
			Sum		**3.29248**		**Sum**		**3.18741**	**Co^{3+}**
3	Co1 - O1*	1.932(2)	1.692	0.37	0.52275		1.680	0.37	0.50607	
	Co1 - O1	1.932(2)	1.692	0.37	0.52275		1.680	0.37	0.50607	
	Co1 – O2	1.899(2)	1.692	0.37	0.57151		1.680	0.37	0.55328	
	Co1 –O2*	1.899(2)	1.692	0.37	0.57151		1.680	0.37	0.55328	
	Co1 - N1*	1.896(3)	1.692	0.37	0.57617		1.680	0.37	0.55778	
	Co1 - N1	1.896(3)	1.692	0.37	0.57617		1.680	0.37	0.55778	
			Sum		**3.34088**		**Sum**		**3.23427**	**Co^{3+}**
4	Co1 - O1*	1.936(3)	1.692	0.37	0.51713		1.680	0.37	0.50062	
	Co1 - O1	1.936(3)	1.692	0.37	0.51713		1.680	0.37	0.50062	
	Co1 – O2	1.899(3)	1.692	0.37	0.57151		1.680	0.37	0.55328	
	Co1 –O2*	1.899(3)	1.692	0.37	0.57151		1.680	0.37	0.55328	
	Co1 - N1*	1.904(4)	1.692	0.37	0.56384		1.680	0.37	0.54585	
	Co1 - N1	1.904(4)	1.692	0.37	0.56384		1.680	0.37	0.54585	
			Sum		**3.30499**		**Sum**		**3.19952**	**Co^{3+}**

Table S3. Bond lengths (Å) found in **1-4**.

Compound 1		Compound 2		Compound 3		Compound 4	
Dy1-O3	2.423(4)	Tb1- O1*	2.388(5)	Ho1-O3	2.421(2)	Er1-O3	2.413(3)
Dy1-O3*	2.423(4)	Tb1- O1	2.388(5)	Ho1-O3*	2.421(2)	Er1-O3*	2.413(3)
Dy1-O1	2.374(4)	Tb1- O3	2.439(5)	Ho1-O1	2.365(2)	Er1-O1	2.355(3)
Dy1-O1*	2.374(4)	Tb1- O3*	2.439(5)	Ho1-O1*	2.365(2)	Er1-O1*	2.355(3)
Dy1-O4*	2.297(4)	Tb1- O4	2.314(5)	Ho1-O4*	2.294(2)	Er1-O4*	2.280(3)
Dy1-O4	2.297(4)	Tb1- O4*	2.314(5)	Ho1-O4	2.294(2)	Er1-O4	2.280(3)
Dy1-O6	2.379(4)	Tb1- O6	2.397(5)	Ho1-O6	2.367(2)	Er1-O6	2.358(3)
Dy1-O6*	2.379(4)	Tb1- O6*	2.397(5)	Ho1-O6*	2.367(2)	Er1-O6*	2.358(3)
Co1-O1*	1.925(4)	Co1-O1*	1.935(5)	Co1-O1*	1.932(2)	Co1-O1*	1.936(3)
Co1-O1	1.925(4)	Co1-O1	1.935(5)	Co1-O1	1.932(2)	Co1-O1	1.936(3)
Co1-O3	1.899(3)	Co1-O2	1.906(5)	Co1-O2	1.899(2)	Co1-O2	1.899(3)
Co1-O3*	1.899(3)	Co1-O2*	1.906(5)	Co1-O2*	1.899(2)	Co1-O2*	1.899(3)
Co1-N1*	1.892(5)	Co1-N1*	1.902(6)	Co1-N1*	1.896(3)	Co1-N1*	1.904(4)
Co1-N1	1.892(5)	Co1-N1	1.902(6)	Co1-N1	1.896(3)	Co1-N1	1.904(4)

Table S4. Bond angles (°) found in **1**.

O3[1] Dy1 Co1	64.15(9)	N1[1] Co1 O1[1]	91.46(19)
O3 Dy1 Co1	64.15(9)	N1[1] Co1 O1	175.2(2)
O3[1] Dy1 O3	128.30(19)	N1 Co1 O1	91.46(19)
O1[1] Dy1 Co1	36.03(9)	N1 Co1 O2	88.30(19)
O1 Dy1 Co1	36.03(9)	N1[1] Co1 O2	89.25(19)
O1[1] Dy1 O3	69.38(13)	N1 Co1 O2[1]	89.25(19)
O1 Dy1 O3	69.32(13)	N1[1] Co1 O2[1]	88.30(19)
O1 Dy1 O3[1]	69.38(13)	N1[1] Co1 N1	84.1(3)
O1[1] Dy1 O3[1]	69.32(13)	O6[1] Dy1 Co1	113.54(12)
O1[1] Dy1 O1	72.06(18)	O6[1] Dy1 O3[1]	77.17(14)
O1 Dy1 O6	81.36(16)	O6[1] Dy1 O3	124.77(15)
O1[1] Dy1 O6[1]	81.36(16)	O6 Dy1 O3	77.17(14)
O1 Dy1 O6[1]	142.77(15)	O6 Dy1 O3[1]	124.78(15)
O1[1] Dy1 O6	142.77(14)	O6[1] Dy1 O6	132.9(2)
O4[1] Dy1 Co1	131.98(10)	O1 Co1 Dy1	46.49(11)
O4 Dy1 Co1	131.98(10)	O1[1] Co1 Dy1	46.49(11)
O4[1] Dy1 O3[1]	74.34(14)	O1[1] Co1 O1	93.0(2)
O4 Dy1 O3	74.34(14)	O2 Co1 Dy1	91.65(13)
O4[1] Dy1 O3	148.56(14)	O2[1] Co1 Dy1	91.65(13)
O4 Dy1 O3[1]	148.56(14)	O2 Co1 O1[1]	89.84(16)
O4[1] Dy1 O1	107.67(14)	O2[1] Co1 O1	89.84(16)
O4 Dy1 O1	141.10(13)	O2[1] Co1 O1[1]	92.44(17)
O4[1] Dy1 O1[1]	141.10(14)	O2 Co1 O1	92.44(17)
O4 Dy1 O1[1]	107.68(14)	O2[1] Co1 O2	176.7(3)
O4[1] Dy1 O4	96.0(2)	O4[1] Dy1 O6[1]	77.47(16)
O4 Dy1 O6[1]	71.50(15)	O4[1] Dy1 O6	71.50(15)
O4 Dy1 O6	77.46(16)	N1 Co1 O1[1]	175.3(2)

Table S5. Bond angles (°) found in **2**.

O1[1] Tb1 Co1	36.04(11)	N1 Co1 O2[1]	88.8(2)
O1 Tb1 Co1	36.04(11)	N1[1] Co1 O2[1]	88.1(2)
O1 Tb1 O1[1]	72.1(2)	N1 Co1 O2	88.1(2)
O1[1] Tb1 O3	69.02(16)	N1 Co1 O1	91.7(2)
O1[1] Tb1 O3[1]	69.32(16)	N1[1] Co1 O1[1]	91.7(2)
O1 Tb1 O3	69.32(16)	N1 Co1 O1[1]	174.8(2)
O1 Tb1 O3[1]	69.03(16)	N1[1] Co1 O1	174.8(2)
O1[1] Tb1 O6	81.47(17)	N1 Co1 N1[1]	83.5(4)
O1[1] Tb1 O6[1]	142.78(17)	C9 O2 Co1	121.4(4)
O1 Tb1 O6	142.78(17)	Co1 O1 Tb1	97.38(19)
O1 Tb1 O6[1]	81.47(17)	O6[1] Tb1 O3[1]	124.71(17)
O3[1] Tb1 Co1	63.91(12)	O6 Tb1 O3[1]	77.46(17)
O3 Tb1 Co1	63.91(11)	O6[1] Tb1 O3	77.47(17)
O3[1] Tb1 O3	127.8(2)	O6 Tb1 O6[1]	132.8(3)
O4[1] Tb1 Co1	132.31(13)	O2[1] Co1 Tb1	92.13(16)
O4 Tb1 Co1	132.30(13)	O6[1] Tb1 O3[1]	124.71(17)
O4 Tb1 O1	107.97(17)	O6 Tb1 O3[1]	77.46(17)
O4[1] Tb1 O1	141.26(17)	O6[1] Tb1 O3	77.47(17)
O4 Tb1 O1[1]	141.26(17)	O2 Co1 Tb1	92.13(16)
O4[1] Tb1 O1[1]	107.96(17)	O2[1] Co1 O2	175.7(3)
O4[1] Tb1 O3	74.70(17)	O2[1] Co1 O1	90.0(2)
O4 Tb1 O3[1]	74.70(17)	O2 Co1 O1	92.9(2)
O4[1] Tb1 O3[1]	148.85(17)	O2 Co1 Tb1	92.13(16)
O4 Tb1 O3	148.86(17)	O2[1] Co1 O2	175.7(3)
O4[1] Tb1 O4	95.4(3)	O2[1] Co1 O1	90.0(2)
O4 Tb1 O6[1]	71.52(17)	O2 Co1 O1[1]	90.0(2)
O4 Tb1 O6	77.15(18)	O2[1] Co1 O1[1]	92.9(2)
O4[1] Tb1 O6	71.52(17)	O1[1] Co1 Tb1	46.58(14)
O4[1] Tb1 O6[1]	77.15(18)	O1 Co1 Tb1	46.57(14)
O6 Tb1 Co1	113.62(13)	O1 Co1 O1[1]	93.2(3)
O6[1] Tb1 Co1	113.62(13)	N1[1] Co1 Tb1	138.3(2)
O6 Tb1 O3	124.71(17)	N1 Co1 Tb1	138.3(2)
O2 Co1 O1[1]	90.0(2)	N1[1] Co1 O2	88.8(2)

Table S6. Bond angles (°) found in **3**.

O1[1] Ho1 Co1	36.26(5)	N1[1] Co1 O2	89.30(10)
O1 Ho1 Co1	36.26(5)	N1 Co1 O2	88.34(10)
O1 Ho1 O1[1]	72.51(10)	N1 Co1 O2[1]	89.30(10)
O1[1] Ho1 O3[1]	69.69(7)	N1[1] Co1 O1	175.31(10)
O1 Ho1 O3	69.69(7)	N1 Co1 O1	91.59(10)
O1 Ho1 O3[1]	69.46(7)	N1 Co1 O1[1]	175.31(10)
O1[1] Ho1 O3	69.46(7)	N1[1] Co1 O1[1]	91.59(10)
O1[1] Ho1 O6	80.92(8)	N1 Co1 N1[1]	84.11(16)
O1[1] Ho1 O6[1]	142.73(7)	C9 O2 Co1	122.0(2)
O1 Ho1 O6	142.73(7)	Co1 O1 Ho1	97.36(8)
O1 Ho1 O6[1]	80.92(8)	O6[1] Ho1 O3[1]	124.42(7)
O3 Ho1 Co1	64.35(5)	O6[1] Ho1 O3	77.13(7)
O3[1] Ho1 Co1	64.35(5)	O6 Ho1 O6[1]	133.39(11)
O3 Ho1 O3[1]	128.70(10)	O2 Co1 Ho1	91.59(7)
O4[1] Ho1 Co1	132.26(6)	O2[1] Co1 Ho1	91.58(7)
O4 Ho1 Co1	132.26(6)	O2 Co1 O2[1]	176.83(13)
O4[1] Ho1 O1	141.12(7)	O2 Co1 O1[1]	89.73(9)
O4 Ho1 O1	107.82(7)	O2 Co1 O1	92.45(9)
O4[1] Ho1 O1[1]	107.82(7)	O2[1] Co1 O1[1]	92.45(9)
O4 Ho1 O1[1]	141.12(7)	O6 Ho1 Co1	113.30(6)
O4[1] Ho1 O3[1]	148.65(7)	O6 Ho1 O3	124.41(7)
O4 Ho1 O3[1]	74.22(7)	O6 Ho1 O3[1]	77.13(7)
O4 Ho1 O3	148.65(7)	O2[1] Co1 O1	89.73(9)
O4[1] Ho1 O3	74.22(7)	O1 Co1 Ho1	46.39(6)
O4[1] Ho1 O4	95.49(11)	O1[1] Co1 Ho1	46.39(6)
O4 Ho1 O6	77.40(8)	O1 Co1 O1[1]	92.77(12)
O4[1] Ho1 O6	71.70(8)	N1[1] Co1 Ho1	137.94(8)
O4 Ho1 O6[1]	71.70(8)	N1 Co1 Ho1	137.95(8)
O4[1] Ho1 O6[1]	77.40(8)	N1[1] Co1 O2[1]	88.34(10)
O6[1] Ho1 Co1	113.31(6)		

Table S7. Bond angles (°) found in **4**.

O1[1] Er1 Co1	36.46(7)	O1[1] Co1 O1	92.63(17)
O1 Er1 Co1	36.46(7)	N1 Co1 Er1	137.91(12)
O1[1] Er1 O1	72.92(14)	N1[1] Co1 Er1	137.91(12)
O1[1] Er1 O3[1]	69.65(10)	N1 Co1 O1	91.62(14)
O1 Er1 O3[1]	70.05(10)	N1[1] Co1 O1	175.35(15)
O1[1] Er1 O3	70.05(10)	N1[1] Co1 O1[1]	91.62(14)
O1 Er1 O3	69.65(10)	N1 Co1 O1[1]	175.36(15)
O1 Er1 O6	80.67(11)	N1[1] Co1 N1	84.2(2)
O1[1] Er1 O6[1]	80.67(11)	Co1 O1 Er1	97.22(12)
O1[1] Er1 O6	142.63(10)	O3[1] Er1 O3	129.28(14)
O1 Er1 O6[1]	142.63(10)	O6[1] Er1 Co1	113.16(8)
O4 Er1 Co1	132.44(8)	O6 Er1 Co1	113.16(8)
O4[1] Er1 Co1	132.44(8)	O6[1] Er1 O3[1]	124.43(10)
O4 Er1 O1	141.26(10)	O6[1] Er1 O3	76.79(10)
O4[1] Er1 O1	107.78(10)	O6 Er1 O3[1]	76.79(10)
O4 Er1 O1[1]	107.78(10)	O6 Er1 O3	124.43(10)
O4[1] Er1 O1[1]	141.26(10)	O6 Er1 O6[1]	133.68(16)
O4 Er1 O4[1]	95.13(15)	O2[1] Co1 Er1	91.75(9)
O4 Er1 O3[1]	74.09(10)	O2 Co1 Er1	91.75(9)
O4[1] Er1 O3	74.09(10)	O2[1] Co1 O2	176.51(19)
O4[1] Er1 O3[1]	148.44(11)	O2 Co1 O1[1]	92.61(12)
O4 Er1 O3	148.43(11)	O2[1] Co1 O1	92.61(12)
O4 Er1 O6[1]	71.88(11)	O2[1] Co1 O1[1]	89.80(12)
O4[1] Er1 O6[1]	77.31(11)	O2 Co1 O1	89.80(12)
O4[1] Er1 O6	71.88(11)	O2 Co1 N1	89.26(14)
O4 Er1 O6	77.31(11)	O2 Co1 N1[1]	88.14(14)
O3[1] Er1 Co1	64.64(7)	O2[1] Co1 N1	88.14(14)
O3 Er1 Co1	64.64(7)	O2[1] Co1 N1[1]	89.26(14)
O1 Co1 Er1	46.32(8)	O1[1] Co1 Er1	46.32(9)

Shape analysis

OP-8 1 D8h Octagon

HPY-8 2 C7v Heptagonal pyramid

HBPY-8 3 D6h Hexagonal bipyramid

CU-8 4 Oh Cube

SAPR-8 5 D4d Square antiprism

TDD-8 6 D2d Triangular dodecahedron

JGBF-8 7 D2d Johnson gyrobifastigium J26

JETBPY-8 8 D3h Johnson elongated triangular bipyramid J14

JBTPR-8 9 C2v Biaugmented trigonal prism J50

BTPR-8 10 C2v Biaugmented trigonal prism

JSD-8 11 D2d Snub diphenoid J84

TT-8 12 Td Triakis tetrahedron

ETBPY-8 13 D3h Elongated trigonal bipyramid

Table S8. Shape analysis for complexes **1-4**

Structure [ML9	Co^{III}-Dy	Co^{III}-Tb	Co^{III}-Ho	Co^{III}-Er
OP-8	28.653	28.559	28.680	28.640
HPY-8	22.493	22.449	22.510	22.567
HBPY-8	15.361	15.350	15.371	15.465
CU-8	8.911	8.837	8.858	8.944
SAPR-8	1.314	1.292	1.229	1.182
TDD-8	**1.127**	**1.136**	**1.110**	**1.086**
JGBF-8	15.324	15.350	15.384	15.436
JETBPY-8	27.333	27.554	27.344	27.312
JBTPR-8	2.771	2.775	2.720	2.653
BTPR-8	2.337	2.342	2.289	2.234
JSD-8	3.488	3.513	3.482	3.409
TT-8	9.426	9.340	9.381	9.461
ETBPY-8	22.356	22.566	22.456	22.515

Structure [ML8] OP-8 HPY-8 HBPY-8 CU-8 SAPR-8 TDD-8 JGBF-8 JETBPY-8 JBTPR-8 BTPR-8 JSD-8 TT-8 ETBPY-8
Co_Dy , 28.653, 22.493, 15.361, 8.911, 1.314, 1.127, 15.324, 27.333, 2.771, 2.337, 3.488, 9.426, 22.356

Structure [ML8] OP-8 HPY-8 HBPY-8 CU-8 SAPR-8 TDD-8 JGBF-8 JETBPY-8 JBTPR-8 BTPR-8 JSD-8 TT-8 ETBPY-8
Co_Tb , 28.559, 22.449, 15.350, 8.837, 1.292, 1.136, 15.350, 27.554, 2.775, 2.342, 3.513, 9.340, 22.566

Structure [ML8] OP-8 HPY-8 HBPY-8 CU-8 SAPR-8 TDD-8 JGBF-8 JETBPY-8 JBTPR-8 BTPR-8 JSD-8 TT-8 ETBPY-8
Co_Ho , 28.680, 22.510, 15.371, 8.858, 1.229, 1.110, 15.384, 27.344, 2.720, 2.289, 3.482, 9.381, 22.456

Structure [ML8] OP-8 HPY-8 HBPY-8 CU-8 SAPR-8 TDD-8 JGBF-8 JETBPY-8 JBTPR-8 BTPR-8 JSD-8 TT-8 ETBPY-8
Co_Er , 28.640, 22.567, 15.465, 8.944, 1.182, 1.086, 15.436, 27.312, 2.653, 2.234, 3.409, 9.461, 22.515

Table S9. List of Co^{III}-Ln^{III} complexes display Single-Ion Magnetic behaviour reported in literature.[1-5]

Molecular formula and ligands	SMMs	Energy barrier (U_{eff}) and relaxation time	Ref.
$[Co^{II}_2(\mu\text{-}OH_2)(O_2CCMe_3)_4(HO_2CCMe_3)_4]$ [where Ln = Dy, for 1; Tb, for 2; Ho, for 3; and Er, for 4] *N,N′*-Bis(salicylidene)ethylenediamine (H_2L)	Y	3.9 K, 1.22×10^{-6} s (for **1**)	this work
$K[Dy\{Co(nta)(m\text{-}ox)\}_2(H_2O)_5]$ (**2**) H_3nta = nitrilotriacetic acid	No	No	1
$[L^1Co(III)Br_2Dy(III)(acac)_2]\cdot CH_2Cl_2$ (**5**), $[L^2Co(III)Cl_2Dy(III)(acac)Cl(MeOH)]$ (6), $[L^2Co(III)Cl_2Dy(III)(acac)Cl(H_2O)]$ (7), $[L^2Co(III)Cl_2Dy(III)(NO_3)_2(MeOH)]$ (8)	Y	167 K, 2.07×10^{-7} s (for **5**), 118 K, 2.90×10^{-7} s (for **6**), 75 K, 3.20×10^{-7} s (for **7**)	2
$[Co^{III}Dy^{III}L^1(\mu\text{-}OAc)_2](NO_3)_2$ [N,N-ethylenebis(3-ethoxysalicylaldimine) =H_2L^1) $[Co^{III}Dy^{III}L^2(\mu\text{-}OAc)_2](NO_3)_2$ [N,N-ethylenebis(3-methoxysalicylaldimine) = H_2L^2]		18 K, 2.5×10^{-6} s	3
$[Co(H_{0.5}L)Dy(DBM)_2H_2O](ClO_4)_{0.5}(H_2O)_3$ H_4L (2,2-[1,2-ethanediylbis[(hydroxyethylimino)methylene]]bis[6-methoxy-4-methyl-phenol]), dibenzoylmethane (HDBM)	Y	88.9 K, 1.34×10^{-10} s	4
$[Co^{III}Dy^{III}(HL)(AcO)_3(H_2O)_3]\cdot(AcO)(H_2O)$	Y	113 K, 7.0×10^{-9} s	5

Computational details:

Ab Initio Calculations. Using MOLCAS 8.2,[6] ab initio calculations were performed on the trivalent lanthanide ions Dy, Tb, Ho, and Er using the single-crystal structural data. Relativistic effects are taken into account on the basis of the Douglas−Kroll.[7] The complete active space self-consistent field (CASSCF) method achieved the spin-free eigenstates.[8] We have employed the [ANO-RCC...8s7p5d3f2g1h] basis set[9] for Dy, Tb, Ho, and Er atoms, the [ANO-RCC...3s2p] basis set for C atoms, the [ANO-RCC...2s] basis set for H atoms, the [ANO-RCC...3s2p1d] basis set for N atoms, and the [ANO-RCC...3s2p1d] basis set for O atoms. The CASSCF calculations that were performed included 9 electrons across 7 4f orbitals of the Dy^{3+} ion, 8 electrons across 7 4f orbitals of the Tb^{3+} ion, 10 electrons across 7 4f orbitals of the Ho^{3+} ion, and 11 electrons across 7 4f orbitals of the Er^{3+} in **1**−**4**, respectively. With this active space, 21 roots in the

configuration interaction (CI) procedure were computed for complex **1**. We also considered 7 septet excited states, 140 quintet excited states, and 195 triplet excited states for complex **2** and 35 quintet excited states, 210 triplet excited states, 195 singlet excited states for complex **3**, and 35 quartet excited states, 212 doublets states for complex **4** in the calculations to compute the anisotropy.

After computing these excited states, we mixed all roots using RASSI-SO;[10] spin−orbit coupling is considered within the space of the calculated spin-free eigenstates for 2, 3, and 4. Moreover, these computed SO states have been considered in the SINGLE_ANISO[11] program to compute the g tensors. Cholesky decomposition for 2-electron integrals has been employed throughout our calculations. Crystal-field parameters have been extracted using the SINGLE_ANISO code, as implemented in MOLCAS 8.2.

References

1. Y. Yamada, M. Tanabe, Y. Miyashita, K.-I. Okamoto, Oxalato-bridged di- and trinuclear Co(III)/Dy(III) complexes derived from mononuclear Co(III) complex with nitrilotriacetate. *Polyhedron* 2003, **22**, 1455-1459. DOI: 10.1016/S0277-5387(03)00122-0.

2. J.-W. Yang, Y.-M. Tian, J. Tao, P. Chen, H.-F. Li, Y.-Q. Zhang, P.-F. Yan, W.-B. Sun, Modulation of the Coordination Environment around the Magnetic Easy Axis Leads to Significant Magnetic Relaxations in a Series of 3d-4f Schiff Complexes, *Inorg. Chem*., 2018, **57**, 8065–8077. DOI: 10.1021/acs.inorgchem.8b00056.

3. S. Hazra, J. Titiš, D. Valigura, R. Boča, S. Mohanta, Bis-phenoxido and bis-acetato bridged heteronuclear {$Co^{III}Dy^{III}$} single molecule magnets with two slow relaxation branches, *Dalton Trans*., 2016, **45**, 7510–7520. DOI: 10.1039/C6DT00848H.

4. M.-J. Liu, J. Yuan, B.-L. Wang, S.-T. Wu, Y.-Q. Zhang, C.-M. Liu, H.-Z. Kou, Spontaneous Resolution of Chiral Co(III)Dy(III) Single-Molecule Magnet Based on an Achiral Flexible Ligand. *Cryst. Growth&Des.* 2018, **18**, 7611−7617. DOI: 10.1021/acs.cgd.8b01410.

5. M. Dolai, M. Ali, J. Titiš, R. Boča, Cu(II)–Dy(III) and Co(III)–Dy(III) based single molecule magnets with multiple slow magnetic relaxation processes in the Cu(II)–Dy(III) complex. *Dalton Trans*., 2015,**44**, 13242–13249. DOI: 10.1039/c5dt00960j.

6. F. Aquilante, T. B. Pedersen, V. Veryazov, R. Lindh, MOLCAS a software for multiconfigurational quantum chemistry calculations, *WIREs Comput. Mol. Sci*., 2013, **3**, 143-149. DOI: 10.1002/wcms.1117.

7. B. A. Hess, C. M. Marian, U. Wahlgren, O. Gropen, A mean field spin-orbit method applicable to correlated wavefunctions, *Chem. Phys. Lett*., 1996, **251**, 365-371. DOI: 10.1016/0009-2614(96)00119-4.

8. B. O. Roos, P.-A. Malmqvist, Relativistic quantum chemistry: the multiconfigurational approach, *Phys. Chem. Chem. Phys*., 2004, **6**, 2919-2927. DOI: 10.1039/B401472N.

9. B. O. Roos, R. Lindh, P.-A. Malmqvist, V. Veryazov, P.-O. Widmark, A. C. Borin, New Relativistic Atomic Natural Orbital Basis Sets for Lanthanide Atoms with Applications to the Ce Diatom and LuF_3, *J. Phys. Chem. A*, 2008, **112**, 11431-11435. DOI: 10.1021/jp803213j.

10. P. A. Malmqvist, B. O. Roos, B. Schimmelpfennig, The restricted active space (RAS) state interaction approach with spin-orbit coupling, *Chem. Phys. Lett*., 2002, **357**, 230-240. DOI: 10.1016/S0009-2614(02)00498-0.

11. L. F. Chibotaru, L. Ungur, Ab initio calculation of anisotropic magnetic properties of complexes. I. Unique definition of pseudospin Hamiltonians and their derivation, *J. Chem. Phys*., 2012, **137**, 064112-22. DOI: 10.1063/1.4739763.